THE JOURNAL OF PHYSICAL CHEMISTRY Letters

Letter

pubs.acs.org/JPCL

Vibrational Signature of Water Molecules in Asymmetric Hydrogen Bonding Environments

Chao Zhang,*[,†] Rustam Z. Khaliullin,[†] Daniele Bovi,[‡] Leonardo Guidoni,*[,‡,§] and Thomas D. Kühne*[,†]

[†]Institute of Physical Chemistry and Center for Computational Sciences, Johannes Gutenberg University Mainz, Staudinger Weg 7, D-55128 Mainz, Germany

[‡]Physics Department, Sapienza - Università di Roma, P.le A. Moro 5, 00185 Rome, Italy

[§]Department of Physical and Chemical Sciences, University of L'Aquila, Via Vetoio, 67100 L'Aquila, Italy

Supporting Information

ABSTRACT: The O−H stretching vibrational modes of water molecules are sensitive to their local environments. Here, we applied effective normal-mode analysis to isolate contributions of each of the two hydrogen atoms to the vibrational modes ν_1 and ν_3 of water molecules in the liquid phase. We demonstrate that the decoupling of the two contributions f_d and the frequency splitting of the vibrational modes $\Delta\omega_{13}$ are inextricably related to the symmetry of the hydrogen bonding environment. We show that ambient liquid water modeled at the density functional level of theory exhibits the characteristics of an asymmetric environment with an average decoupling of 0.82 and a splitting of 137 inverse centimeters. Such large value of decoupling and splitting would account for the inhomogeneous broadening as observed in the vibrational spectra of liquid water. The computational protocols and the results of this work will facilitate the interpretation of experimental Raman and infrared spectra of interfacial water molecules at hydrophobic, membrane, and protein surface.

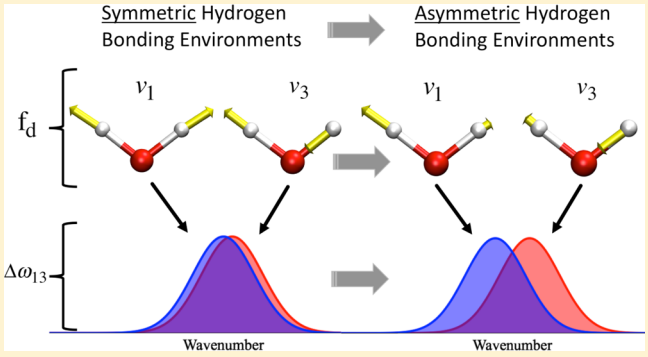

SECTION: Liquids; Chemical and Dynamical Processes in Solution

The properties and behavior of liquid water have been a subject of scientific investigation for many centuries.[1] Since the early works on the molecular structure of water, it has been accepted that a water molecule in the liquid phase at ambient conditions is bonded, on average, to four neighbors in a distorted tetrahedral configuration.[2,3] This view is based on X-ray and neutron diffraction experiments,[4−6] vibrational spectroscopy,[7−10] thermodynamical data,[2,3] and molecular dynamics simulations.[11−16] However, this traditional picture has recently been questioned based on data from X-ray absorption, X-ray emission, and X-ray Raman scattering experiments.[17] The X-ray spectroscopic features of liquid water have been interpreted as evidence for a large fraction of molecules forming only two strong hydrogen bonds (HBs) in highly asymmetric environments. However, the "rings and chains" structure of liquid water implied by such an interpretation has been challenged on many fronts.[3,18,19]

Recently, Kühne and Khaliullin have applied the energy decomposition analysis based on absolutely localized molecular orbitals (ALMO EDA)[20] to measure the strength of donor−acceptor interactions of individual HBs in liquid water.[21] The ALMO EDA has revealed that even small geometric distortions of HBs cause a substantial change in their strength. Hence, the authors concluded that, although the geometric distortions are not large enough to justify the drastic "chain and ring" model, the majority of water molecules exhibit a significant asymmetry in the strength of their HBs. They have also established that the distortions responsible for the asymmetry appear as fluctuations on a time scale of hundreds of femtoseconds.

Vibrational motions of water molecules have a characteristic time scale of 10 to 100 fs, which corresponds to the spectroscopic range of 300−4000 cm^{-1}.[22] Since intramolecular O−H stretching vibrations occur on a significantly shorter time scale than the asymmetry relaxation described by Kühne and Khaliullin,[21] they represent excellent probes for detecting distorted hydrogen bonding environments.[23] Indeed, vibrational spectra of liquid water, such as Raman and infrared (IR), exhibit a large red shift in the frequencies of O−H stretching modes compared to those in the gas phase. In particular, IR spectra have a board continuum that spans the range from 3000 cm^{-1} to 3700 cm^{-1}, with a center at around 3400 cm^{-1}, while Raman spectra show isosbestic points.[24]

The inhomogeneous broadening in vibrational spectra has become a subject of many theoretical investigations. Valuable insights have been provided by combining classical molecular

Received: June 27, 2013
Accepted: September 12, 2013
Published: September 12, 2013

dynamics (MD) simulations and quantum mechanical theory.[25−37] A variety of factors contributing to the broadening have been pointed out, such as hydrogen bonding configurations,[25,33,34] bending overtune,[35] intermolecular vibration[26−29,36,37] as well as coupling of symmetric and asymmetric local modes.[32] To gain a deeper insight, it would be desirable to include both the electronic and nuclear degrees of freedom on an equal footing and treat the intra- and intermolecular O−H vibration simultaneously. Ab initio MD, where the molecular interactions are calculated "on the fly", is a powerful tool to investigate the vibrational spectra of liquid water.[38−41] Indeed, it has been shown from ab initio MD simulations that charge fluctuations would be an important factor for the inhomogeneous broadening in Raman spectra.[42]

In this Letter, we combine the strengths of ab initio MD,[43,44] effective normal modes analysis,[45,46] and ALMO EDA[20] to investigate vibrational signatures of water molecules in asymmetric hydrogen bonding environments. In particular, we characterize the local hydrogen bonding asymmetry of each water molecule by the contributions of individual O−H vibrations to the stretching modes ν_1 and ν_3 and relate it to the corresponding frequency splitting of ω_1 and ω_3. Effective normal mode ν_k of each water molecule can be extracted from its vibrational density of states (VDOS) by minimizing the following functional:

$$\Omega^{(n)} = \sum_k \left(\frac{\beta}{2\pi} \int d\omega\, |\omega|^{2n} P^{\nu_k}(\omega) - \left(\frac{\beta}{2\pi} \int d\omega\, |\omega|^{n} P^{\nu_k}(\omega) \right)^2 \right) \quad (1)$$

with respect to ν_k. Here β is the inverse temperature, n is an integer constant, and P^{ν_k} is the VDOS of ν_k. For $n = 2$, this method is equivalent to a normal-mode analysis performed with the thermally averaged Hessian matrix.[45] The contribution of the internal coordinates x_i (such as bond distances and angles) to ν_k is denoted as C_{kj}[47−49] and can be easily obtained after the minimization procedure. As shown later, this information is very important and can be utilized to define the local hydrogen bonding asymmetry. To illustrate this, we first briefly describe a textbook example of coupled harmonic oscillators (Scheme 1).

Scheme 1. Coupled Harmonic Oscillators with Mass m and Restoring Force Constants k_1, k_2, and k'

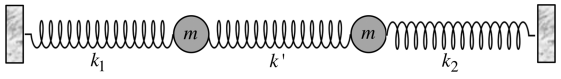

In this system, if the restoring force constants are equal (i.e., $k_1 = k_2$), the normal modes of the system are [1,1] for the symmetric stretching mode and [−1,1] for the asymmetric stretching mode. This case represents a symmetric environment, where both oscillators are perfectly coupled. When $k_1 \neq k_2$, these two normal modes become $[\delta + (1 + \delta^2)^{1/2},1]$ and $[\delta - (1 + \delta^2)^{1/2},1]$ respectively, where $\delta = (k_2 - k_1)/2k'$. Thus, the asymmetry in the restoring force constants leads to a decoupling of the two vibrations, where the degree of decoupling depends on the difference between k_1 and k_2. In addition, the splitting of the corresponding normal frequencies $\Delta\omega_{13} \propto 1 + \delta^2$ becomes larger in this case (see Supporting Information, Section A for details).

This simple example implies that asymmetric hydrogen bonding environments might significantly affect the relative contributions of the two intramolecular O−H bonds, further denoted as O−H1 and O−H2, to the symmetric and asymmetric stretching modes ν_1 and ν_3 of each water molecule. This provides a possibility to characterize the hydrogen bonding asymmetry with the degree of decoupling f_d between the O−H1 and O−H2 vibrations:

$$f_d = \sum_{k=\nu_1,\nu_3} \frac{|C_{kO-H1} - C_{kO-H2}|}{2(C_{kO-H1} + C_{kO-H2})} \quad (2)$$

where C_{kO-H1} and C_{kO-H2} are contributions of O−H1 and O−H2 bonds to the effective normal mode k, respectively. When f_d equals 0, the two O−H bonds are completely coupled in their motions, and water molecules are in fully symmetric hydrogen bonding environments. When f_d equals 1, the two O−H bonds are completely decoupled in their motions, and water molecules are in fully asymmetric hydrogen bonding environments. The example of coupled harmonic oscillators model also show that asymmetric hydrogen bonding environments might also have a substantial impact on the corresponding frequency splitting $\Delta\omega_{13}$.

This hypothesis was tested with ab initio simulations. Four model systems were utilized to understand the effect of the hydrogen bonding environment on the vibrational modes: water monomer at 0 K (system **A**), water monomer at 300 K (system **B**), water dimer at 0 K (system **C**) and liquid water at 300 K (system **D**). The electronic structure problem was solved within the framework of density functional theory (DFT) using the Perdew−Burke−Ernzerhof (PBE) exchange and correlation (XC) functional[50] as implemented in the CP2K suite of programs.[51] Within CP2K, a dual basis of Gaussian-type orbitals and plane waves was utilized.[52] We used an accurate triple-ζ basis set with two additional sets of polarization functions (TZV2P). The electronic charge density was expanded in terms of plane waves with a density cutoff of 320 Ry. The dual-space Goedecker−Teter−Hutter pseudopotentials[53] were used to account for the core electrons. The simulation box for all gas-phase systems (systems **A**, **B**, and **C**) was set to 15.7 Å × 15.7 Å × 15.7 Å and a Poisson solver for isolated systems was employed.[54] For system **D**, a periodic simulation cell consisting of 128 light water molecules with a density of 0.9966 g/cm^3 was employed. For systems **B** and **D**, we took advantage of the efficient and accurate second-generation Car−Parrinello MD simulation method,[44] with an integration time-step of 0.5 fs. Even though ordinary DFT-PBE water at ambient conditions is somewhat overstructured and less fluid than real water,[15,55] previous work has shown that this setup yields a qualitatively correct description of the structure, diffusion, and vibrational spectrum of liquid water.[56] Furthermore, recent investigations showed that van der Waals interactions are important in describing the structure and dynamics of liquid water;[57−59] however, its effects are less dramatic in NVT simulations, where the density is fixed and set to the experimental value (as in our case), than those in NPT simulations. For system **B**, the trajectory was accumulated for 20 ps, while for system **D**, an ab initio MD simulation of 80 ps was carried out, and the last 60 ps were used for the analysis. In order to perform the effective normal modes analysis, we subdivided the ab initio MD trajectories of each water molecule in system **D** into 2 ps windows, which correspond roughly to the HB lifetime in liquid water[60] and less than the HB lifetime

dx.doi.org/10.1021/jz401321x | J. Phys. Chem. Lett. 2013, 4, 3245−3250

(6.99 ps) and water residence time (7.25 ps) estimated from our simulations (see Supporting Information Section B for details). This procedure provided a total of 3840 configurations of individual water molecules for the effective normal modes analysis.

The normal modes of a water monomer at 0 K are shown in Figure 1A, where O−H1 and O−H2 are fully coupled (i.e., the hydrogen atoms move together with the same amplitudes). This indicates that the water monomer in vacuum experiences a symmetric environment with no intermolecular interactions. At 300 K (Figure 1B), O−H1 and O−H2 remain fully coupled with f_d = 0.01. This suggests that (i) the temperature and anharmonicity alone have only negligible effects on these modes, and (ii) eq 1 is appropriate for the vibrational analysis at finite temperature.

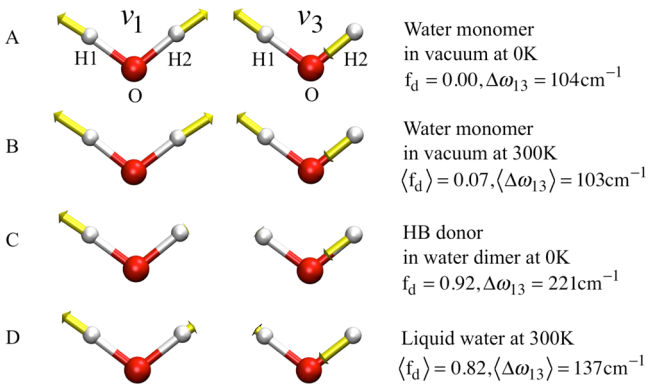

Figure 1. The symmetric and asymmetric stretching modes ν_1 and ν_3 of a water molecule (A) in vacuum at 0 K, (B) in vacuum at 300 K, (C) as the HB donor of the water dimer at 0 K, and (D) in liquid water at 300 K. f_d represents the difference in contributions of O−H1 and O−H2 to the symmetric and asymmetric stretching modes ν_1 and ν_3. $\Delta\omega_{13}$ is the frequency splitting between ν_1 and ν_3.

Next, we analyzed the vibrational characteristics of the HB donor of the water dimer in vacuum at 0 K (Figure 1C), which represents a water molecule in a simple asymmetric hydrogen bonding environment: O−H1 forms an HB, whereas O−H2 does not. In this case, O−H1 and O−H2 of an HB donor are almost completely decoupled with f_d = 0.92. In addition, we find that $\Delta\omega_{13}$ increases from 104 cm^{-1} for the water monomer in vacuum at 0 K to 221 cm^{-1}. All these observations enforce the hypothesis that f_d and $\Delta\omega_{13}$ are excellent descriptors to distinguish the symmetry of the environment of a water molecules.

The effective normal modes analysis of liquid water reveals that the vibrational motions of O−H1 and O−H2 in liquid water are largely decoupled with $\langle f_d \rangle$ = 0.82. These modes resemble those of the HB donor in the water dimer (Figure 1D). Interestingly, they also share similarities with the instantaneous normal modes of water molecules at the water/vapor interface.[61]

Since liquid water is famous for its structural complexity, the averages over all states provides only an oversimplified picture. Therefore, we analyzed the distribution of water molecules according to their $f_d - \Delta\omega_{13}$ values (Figure 2) to obtain a more detailed description. As expected, there is a clear positive correlation between $\Delta\omega_{13}$ and f_d. Indeed, the expression $\Delta\omega_{13} \propto 1 + f_d^2$ derived from the coupled harmonic oscillators model (see Supporting Information Section A and Figure S1) also works for liquid water for f_d less than 0.8. When O−H1 and

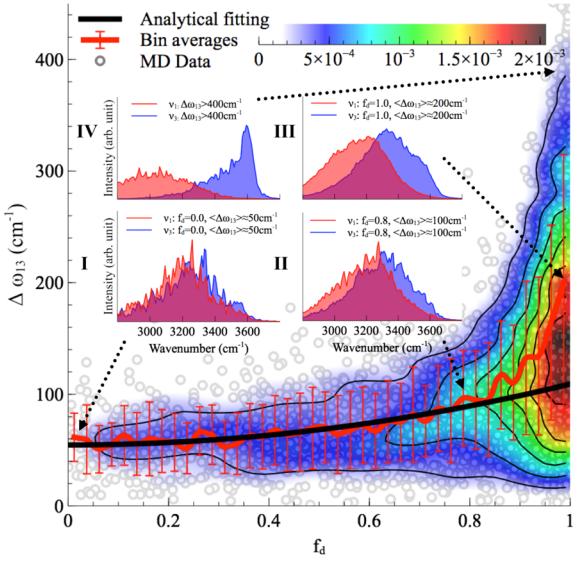

Figure 2. The normalized joint distribution of vibrational descriptors $f_d - \Delta\omega_{13}$ for liquid water. $\langle \Delta\omega_{13} \rangle$ as a function of f_d is also shown. Error bars denote the standard deviation σ of $\langle \Delta\omega_{13} \rangle$ for each value of f_d with a bin size of 0.025. The continuous line has been obtained by fitting the data of $\langle \Delta\omega_{13} \rangle$ with the expression $\Delta\omega_{13} \propto 1 + f_d^2$, as reported in Supporting Information Section A. Insets I−IV denote the vibrational spectra of the symmetric and asymmetric stretching modes ν_1 and ν_3 of the four representative regions in the $(f_d,\Delta\omega_{13})$ space. Each region contains configurations within $[f_d - 0.025, f_d + 0.025]$and $[\langle \Delta\omega_{13} \rangle_{f_d} - \sigma, \langle \Delta\omega_{13} \rangle_{f_d} + \sigma]$. The corresponding vibrational spectra of ν_1 and ν_3 are the averages of the decomposed vibrational density of states of configurations within each region. See Supporting Information Section C and Figure S4 for the calculated full VDOS and IR spectra in comparison with experiments.

O−H2 are fully coupled (i.e., $f_d \approx 0$), $\langle \Delta\omega_{13} \rangle$ is about 50 cm^{-1}. It increases to about 200 cm^{-1} when O−H1 and O−H2 are fully decoupled (i.e., $f_d \approx 1$).

$\Delta\omega_{13}$ of water molecules is not only subject to theoretical calculations but also experimental measurements in both gas[62,63] and condensed phase environments.[64−66] It is also available in experiments for other molecules with C_{2v} molecular symmetry.[67] The values between 50 cm^{-1} and 200 cm^{-1} as we found in liquid water cover almost the entire range of available experimental information. In symmetric environments, $\Delta\omega_{13}$ has been measured around 45 cm^{-1} for water molecules isolated in D_2O cubic ice,[64] 99 cm^{-1} for a water monomer in the gas phase,[62] 95 cm^{-1} for an HB acceptor in the water dimer[63] and 92 cm^{-1} for a water monomer in the hydrophobic liquid CCl_4.[65] In more asymmetric environments, $\Delta\omega_{13}$ becomes larger: 133 cm^{-1} for an HB donor molecule in the water dimer,[63] 225 cm^{-1} for water molecules at the water/CCl_4 interface[65] and 230 cm^{-1} for water molecules at the water/*n*-alkane interface.[66] The average $\langle \Delta\omega_{13} \rangle$ obtained in our simulations of liquid water is about 137 cm^{-1}, which corresponds to a more asymmetric environment.

It is interesting to investigate how the vibrational spectra of ν_1 and ν_3 change at different values of $\langle \Delta\omega_{13} \rangle$. For this purpose, we selected four representative regions of the two-dimensional $f_d - \Delta\omega_{13}$ space (insets I−IV in Figure 2). We note that the calculated full VDOS and IR spectra are in qualitative agreement with experiments (see Supporting Information Section C and Figure S4 for details), even though it is known that the calculated IR with PBE functional has a

dx.doi.org/10.1021/jz401321x | J. Phys. Chem. Lett. 2013, 4, 3245−3250

systemic blue shift in O−H region.[68] Therefore, we focus our analyses on VDOS here. In the symmetric region ($f_d \approx 0, \langle\Delta\omega_{13}\rangle \approx 50$ cm^{-1}), ν_1 and ν_3 are strongly overlapping with a center at around 3220 cm^{-1} (inset I in Figure 2) This coincides with the so-called "ice-like" bands.[69] In the asymmetric region ($f_d \approx 1$, $\langle\Delta\omega_{13}\rangle \approx 200$ cm^{-1}), the overlap between ν_1 and ν_3 is significantly reduced, and two distinct peaks at around 3150 cm^{-1} and 3350 cm^{-1} appear (inset III in Figure 2). The latter is in agreement with the "liquid-like" bands.[69] It is worth mentioning that the majority of water molecules fall into this region of the $f_d - \Delta\omega_{13}$ space. Such a large value of decoupling and splitting would account for the inhomogeneous broadening as observed in the vibrational spectra of liquid water. It is noteworthy to mention that our findings are in accord with a recent computational study of IR spectra of liquid water,[32] which shows that the sum of bands obtained from symmetric and asymmetric basis modes ν_1 and ν_3 reproduces the full spectra, and $\langle\Delta\omega_{13}\rangle$ is about 173.4 cm^{-1}. Furthermore, there are numerous data points with an extremely large split $\Delta\omega_{13} >$ 400 cm^{-1} in Figure 2. These points correspond to a situation in which the peaks of the nonoverlapping ν_1 and ν_3 lie around 3000 cm^{-1} and 3600 cm^{-1}, respectively (inset IV in Figure 2). Remarkably, the latter band resembles that of free dangling O−H bonds at the water/vapor interface.[69,70]

To understand the origins behind the wide range of $\Delta\omega_{13}$ and f_d in liquid water, we analyzed the geometry of the two neighboring HB accepting molecules in the representative (f_d,$\Delta\omega_{13}$) regions (insets I−IV in Figure 2). The indices of the closest neighbors were obtained using the interaction energies of individual HBs obtained with ALMO EDA.[20] ALMO EDA was performed for the configurations collected with an interval of 40 fs for each 2-ps piece of the MD trajectory. Here, we are interested in the energies of two HBs $H_D\cdots O_A$ formed by a water molecule via its two hydrogen atoms, where D stands for a water molecule, which donates its hydrogen atom to its neighbor A. For each water molecule D, sorting the neighbors according to the strength of their interactions enables us to find the strongest and the second strongest HB acceptors A. Subsequently, the distances between the oxygen atoms of D and A (denoted simply as R) and the mutual orientations of the two molecules $\alpha(\angle H_D O_D O_A)$ are calculated for each of the two neighbors (Figure 3).

Figure 3I shows that, in the symmetric region of the vibrational space ($f_d \approx 0, \langle\Delta\omega_{13}\rangle \approx 50$ cm^{-1}), HBs formed by both H1 and H2 have almost identical geometries. Furthermore, their geometric parameters lie within the characteristic HB boundary derived from the minimum energy path of the 2D potential of mean force (PMF)[71] and the commonly used angle cutoff of 30° for the definition of HB. With an increase of $\Delta\omega_{13}$ and f_d, the HB parameters of H2 start to deviate from those of H1: the intermolecular distance R increases and the HBs becomes more distorted (Figure 3II−III). This is direct evidence that water molecules in liquid experience asymmetry in their first coordination shells. For the region $\Delta\omega_{13} >$ 400 cm^{-1} (Figure 3IV), HB parameters of H2 cross the HB boundary, indicating that some HBs are broken. In this case, a water molecule is in a highly asymmetric environment, resembling that of the HB donor in the water dimer or that of the first-layer water molecules at the water surface. Conceivably, that is the reason why the corresponding vibrational frequency of O−H2 or ν_3, as shown in Figure 2 inset IV, could reach 3600 cm^{-1} (the vibration of O−H2 and ν_3 are interchangeable here because the O−H1 and O−H2 are fully decoupled, and contribution of O−H2 to ν_3 is nearly 100%).

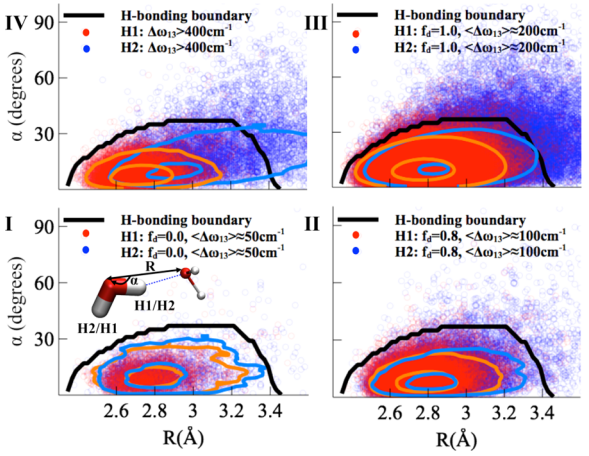

Figure 3. Joint distribution functions of the HB parameters R and α for the four representative (f_d,$\Delta\omega_{13}$) regions in Figure 2. Here, H1 corresponds to the hydrogen atom forming the strongest HB, while H2 corresponds to the hydrogen atom forming a weaker HB. This unambiguous assignment comes from ALMO EDA (see text for details). Contour lines (orange and light blue for H1 and H2, respectively) are based on normalized distributions with levels at 0.0005 and 0.005. α is the angle $\angle H_D O_D H_A$, where D and A stand for HB donor and acceptor, respectively. R is the distance between O_D and O_A. The HB boundary was determined previously as the minimum energy path of the two-dimensional PMF map.[71]

To summarize, we applied ab initio MD simulation and effective normal modes analysis to investigate the relation between the local hydrogen bonding asymmetry and vibrational spectra. In analogy with the coupled harmonic oscillators model, we have introduced a local hydrogen bonding asymmetry descriptor f_d through the contribution of the O−H1 and O−H2 vibrations to the stretching modes ν_1 and ν_3 of each water molecule and related it to the frequency splitting $\Delta\omega_{13}$. An increase of both f_d and $\Delta\omega_{13}$ is a vibrational signature of water molecules in asymmetric environments. At the DFT-PBE level of theory, our model of liquid water has $\langle f_d\rangle \approx 0.82$ and $\langle\Delta\omega_{13}\rangle \approx 137$ cm^{-1} with the majority having stretching modes ν_1 at ∼3150 cm^{-1} and ν_3 at ∼3350 cm^{-1}. The established relation between descriptors f_d,$\Delta\omega_{13}$ and geometric characteristics of HBs via ALMO EDA assignments implies that the distortions of HBs are responsible for the observed strong local asymmetry and frequency splitting. The inhomogeneous broadening of observed vibrational spectra at around 3400 cm^{-1} in liquid water would come as a result of such large value of $\langle f_d\rangle$ and $\langle\Delta\omega_{13}\rangle$. The procedure proposed in this Letter is general and applicable to other systems, such as interfacial water molecules and aqueous solutions. Similar results would be also observed for molecules with the C_{2v} molecular symmetry that form HBs in the liquid phase or in solutions.

■ ASSOCIATED CONTENT

Ⓢ Supporting Information

Relationship between $\Delta\omega_{13}$ and f_d in the coupled harmonic oscillators model, estimations of the hydrogen-bond (HB) lifetime τ_{HB} and residence time τ_{res} of the water molecules in liquid water, and comparison of the calculated and experimental infrared (IR) spectra of liquid water. This material is available free of charge via the Internet http://pubs.acs.org.

dx.doi.org/10.1021/jz401321x | J. Phys. Chem. Lett. 2013, 4, 3245−3250

AUTHOR INFORMATION

Corresponding Authors

*E-mail: zhangc@uni-mainz.de.
*E-mail: leonardo.guidoni@univaq.it.
*E-mail: kuehne@uni-mainz.de.

Notes

The authors declare no competing financial interest.

ACKNOWLEDGMENTS

C.Z. and T.D.K. gratefully acknowledge the Gauss Center for Supercomputing (GCS) for providing computing time through the John von Neumann Institute for Computing (NIC) on the GCS share of the supercomputer JUQUEEN at the Jülich Supercomputing Centre (JSC). Financial support from the Graduate School of Excellence MAINZ and the IDEE project of the Carl-Zeiss Foundation is kindly acknowledged. R.Z.K. is grateful to the Swiss National Science Foundation for financial support and to the Swiss National Supercomputing Centre (CSCS) for computer time.

REFERENCES

(1) Ball, P. Water as an Active Constituent in Cell Biology. *Chem. Rev.* **2008**, *108*, 74−108.
(2) Stillinger, F. H. Water Revisited. *Science* **1980**, *209*, 451−457.
(3) Clark, G. N. I.; Cappa, C. D.; Smith, J. D.; Saykally, R. J.; Head-Gordon, T. The Structure of Ambient Water. *Mol. Phys.* **2010**, *108*, 1415−1433.
(4) Soper, A. K. The Radial Distribution Functions of Water and Ice from 220 to 673 K and at Pressures up to 400 MPa. *Chem. Phys.* **2000**, *258*, 121−137.
(5) Head-Gordon, T.; Hura, G. Water Structure from Scattering Experiments and Simulation. *Chem. Rev.* **2002**, *102*, 2651−2669.
(6) Hura, G.; Russo, D.; Glaeser, R. M.; Head-Gordon, T.; Krack, M.; Parrinello, M. Water Structure as a Function of Temperature from X-ray Scattering Experiments and Ab Initio Molecular Dynamics. *Phys. Chem. Chem. Phys.* **2003**, *5*, 1981−1991.
(7) Fecko, C. J.; Eaves, J. D.; Loparo, J. J.; Tokmakoff, A.; Geissler, P. L. Ultrafast Hydrogen-bond Dynamics in the Infrared Spectroscopy of Water. *Science* **2003**, *301*, 1698−1702.
(8) Eaves, J. D.; Loparo, J. J.; Fecko, C. J.; Roberts, S. T.; Tokmakoff, A.; Geissler, P. L. Hydrogen Bonds in Liquid Water are Broken only Fleetingly. *Proc. Natl. Acad. Sci. U.S.A.* **2005**, *102*, 13019−13022.
(9) Smith, J. D.; Cappa, C. D.; Wilson, K. R.; Cohen, R. C.; Geissler, P. L.; Saykally, R. J. Unified Description of Temperature-Dependent Hydrogen-Bond Rearrangements in Liquid Water. *Proc. Natl. Acad. Sci. U.S.A.* **2005**, *102*, 14171−14174.
(10) Bakker, H.; Skinner, J. Vibrational Spectroscopy as a Probe of Structure and Dynamics in Liquid Water. *Chem. Rev.* **2010**, *110*, 1498−1517.
(11) Todorova, T.; Seitsonen, A. P.; Hutter, J.; Kuo, I. F.; Mundy, C. J. Molecular Dynamics Simulation of Liquid Water: Hybrid Density Functionals. *J. Phys. Chem. B* **2006**, *110*, 3685−3691.
(12) Lee, H.; Tuckerman, M. Structure of Liquid Water at Ambient Temperature from Ab Initio Molecular Dynamics Performed in the Complete Basis Set Limit. *J. Chem. Phys.* **2006**, *125*, 154507.
(13) Paesani, F.; Voth, G. A. The Properties of Water: Insights from Quantum Simulations. *J. Phys. Chem. B* **2009**, *113*, 5702−5719.
(14) Morrone, J.; Car, R. Nuclear Quantum Effects in Water. *Phys. Rev. Lett.* **2008**, *101*, 17801.
(15) Kühne, T. D.; Krack, M.; Parrinello, M. Static and Dynamical Properties of Liquid Water from First Principles by a Novel Car−Parrinello-like Approach. *J. Chem. Theory Comput.* **2009**, *5*, 235−241.
(16) Montagna, M.; Sterpone, F.; Guidoni, L. Structural and Spectroscopic Properties of Water around Small Hydrophobic Solutes. *J. Phys. Chem. B* **2012**, *116*, 11695−11700.
(17) Wernet, P.; Nordlund, D.; Bergmann, U.; Cavalleri, M.; Odelius, M.; Ogasawara, H.; Naslund, L. A.; Hirsch, T. K.; Ojamae, L.; Glatzel, P.; Pettersson, L. G. M.; Nilsson, A. The Structure of the First Coordination Shell in Liquid Water. *Science* **2004**, *304*, 995−999.
(18) Nilsson, A.; Pettersson, L. G. M. Perspective on the Structure of Liquid Water. *Chem. Phys.* **2011**, *389*, 1−34.
(19) Herrmann, A.; Schmidt, W. G.; Schwertfeger, P. *Phys. Rev. Lett.* **2006**, *96*, 016404.
(20) Khaliullin, R. Z.; Cobar, E. A.; Lochan, R. C.; Bell, A. T.; Head-Gordon, M. Unravelling the Origin of Intermolecular Interactions Using Absolutely Localized Molecular Orbitals. *J. Phys. Chem. A* **2007**, *111*, 8753−8765.
(21) (a) Kühne, T. D.; Khaliullin, R. Z. Electronic Signature of the Instantaneous Asymmetry in the First Coordination Shell of Liquid Water. *Nat. Commun.* **2013**, *4*, 1450. (b) Khaliullin, R. Z.; Kühne, T. D. Microscopic Properties of Liquid Water from Combined Ab Initio Molecular Dynamics and Energy Decomposition Studies. *Phys. Chem. Chem. Phys.* **2013**, *15*, 15746−15766.
(22) Wilson, E. B. *Molecular Vibrations: The Theory of Infrared and Raman Vibrational Spectra*; McGraw-Hill: New York, 1955.
(23) Geissler, P. L. Water Interfaces, Solvation, and Spectroscopy. *Annu. Rev. Phys. Chem.* **2013**, *64*, 317−337.
(24) Gopalakrishnan, S.; Liu, D.-F.; Allen, H. C.; Kuo, M.; Shultz, M. J. Vibrational Spectroscopic Studies of Aqueous Interfaces: Salts, Acids, Bases, and Nanodrops. *Chem. Rev.* **2006**, *106*, 1155−1175.
(25) Auer, B.; Kumar, R.; Schmidt, J. R.; Skinner, J. L. Hydrogen Bonding and Raman, IR, and 2D-IR Spectroscopy of Dilute HOD in Liquid D_2O. *Proc. Natl. Acad. Sci. U.S.A.* **2007**, *104*, 14215.
(26) Auer, B. M.; Skinner, J. L. IR and Raman Spectra of Liquid Water: Theory and Interpretation. *J. Chem. Phys.* **2008**, *128*, 224511.
(27) Torii, H. Time-domain Calculations of the Polarized Raman Spectra, the Transient Infrared Absorption Anisotropy, and the Extent of Delocalization of the OH Stretching Mode of Liquid Water. *J. Phys. Chem. A* **2006**, *110*, 9469−9477.
(28) Paarmann, A.; Hayashi, T.; Mukamel, S.; Miller, R. J. D. Probing Intermolecular Couplings in Liquid Water with Two-Dimensional Infrared Photon Echo Spectroscopy. *J. Chem. Phys.* **2008**, *128*, 191103.
(29) Paarmann, A.; Hayashi, T.; Mukamel, S.; Miller, R. J. D. Nonlinear Response of Vibrational Excitons: Simulating the Two-Dimensional Infrared Spectrum of Liquid Water. *J. Chem. Phys.* **2009**, *130*, 204110.
(30) Paesani, F.; Xantheas, S. S.; Voth, G. A. Infrared Spectroscopy and Hydrogen-Bond Dynamics of Liquid Water from Centroid Molecular Dynamics with an Ab Initio-Based Force Field. *J. Phys. Chem. B* **2009**, *113*, 13118−13130.
(31) Paesani, F.; Voth, G. A. A Quantitative Assessment of the Accuracy of Centroid Molecular Dynamics for the Calculation of the Infrared Spectrum of Liquid Water. *J. Chem. Phys.* **2010**, *132*, 014105.
(32) Choi, J. H.; Cho, M. Computational IR Spectroscopy of Water: OH Stretch Frequencies, Transition Dipoles, and Intermolecular Vibrational Coupling Constants. *J. Chem. Phys.* **2013**, *138*, 174108.
(33) Lawrence, C. P.; Skinner, J. L. Vibrational Spectroscopy of HOD in Liquid D_2O. II. Infrared Line Shapes and Vibrational Stokes Shift. *J. Chem. Phys.* **2002**, *117*, 8847−8854.
(34) Moller, K. B.; Rey, R.; Hynes, J. T. Hydrogen Bond Dynamics in Water and Ultrafast Infrared Spectroscopy: A Theoretical Study. *J. Phys. Chem. A* **2004**, *108*, 1275−1289.
(35) Rey, R.; Moller, K. B.; Hynes, J. T. Hydrogen Bond Dynamics in Water and Ultrafast Infrared Spectroscopy. *J. Phys. Chem. A* **2002**, *106*, 11993−11996.
(36) Buch, V. Molecular Structure and OH-Stretch Spectra of Liquid Water Surface. *J. Phys. Chem. B* **2005**, *109*, 17771−17774.
(37) Sadlej, J.; Buch, V.; Kazimirski, J. K.; Buck, U. Theoretical Study of Structure and Spectra of Cage Clusters $(H_2O)_n$, n = 7−10. *J. Phys. Chem. A* **1999**, *103*, 4933−4947.
(38) Kuo, I.-F. W.; Mundy, C. An Ab Initio Molecular Dynamics Study of the Aqueous Liquid−Vapor Interface. *Science* **2004**, *303*, 658.

(39) Sharma, M.; Resta, R.; Car, R. Intermolecular Dynamical Charge Fluctuations in Water: A Signature of the H-Bond Network. *Phys. Rev. Lett.* **2005**, *95*, 187401.
(40) Lee, H.-S.; Tuckerman, M. E. Dynamical Properties of Liquid Water from Ab Initio Molecular Dynamics Performed in the Complete Basis Set Limit. *J. Chem. Phys.* **2007**, *126*, 164501.
(41) Zhang, C.; Donadio, D.; Galli, G. First-Principle Analysis of the IR Stretching Band of Liquid Water. *J. Phys. Chem. Lett.* **2010**, *1*, 1398−1402.
(42) Wan, Q.; Spanu, L.; Galli, G. A.; Gygi, F. Raman Spectra of Liquid Water from Ab Initio Molecular Dynamics: Vibrational Signatures of Charge Fluctuations in the Hydrogen Bond Network. *J. Chem. Theory Comput.* **2013**, *9*, 4124−4130.
(43) Car, R.; Parrinello, M. Unified Approach for Molecular-Dynamics and Density-Functional Theory. *Phys. Rev. Lett.* **1985**, *55*, 2471−2474.
(44) Kühne, T. D.; Krack, M.; Mohamed, F. R.; Parrinello, M. Efficient and Accurate Car−Parrinello-like Approach to Born−Oppenheimer Molecular Dynamics. *Phys. Rev. Lett.* **2007**, *98*, 066401.
(45) Martinez, M.; Gaigeot, M. P.; Borgis, D.; Vuilleumier, R. Extracting Effective Normal Modes from Equilibrium Dynamics at Finite Temperature. *J. Chem. Phys.* **2006**, *125*, 144106.
(46) Bovi, D.; Mezzetti, A.; Vuilleumier, R.; Gaigeot, M.-P.; Chazallon, B.; Spezia, R.; Guidoni, L. Environmental Effects on Vibrational Properties of Carotenoids: Experiments and Calculations on Peridinin. *Phys. Chem. Chem. Phys.* **2011**, *13*, 20954−20964.
(47) Gaigeot, M.-P.; Martinez, M.; Vuilleumier, R. Infrared Spectroscopy in the Gas and Liquid Phase from First Principle Molecular Dynamics Simulations: Application to Small Peptides. *Mol. Phys.* **2007**, *105*, 2857−2878.
(48) Morino, Y.; Kuchitsu, K. A Note on the Classification of Normal Vibrations of Molecules. *J. Chem. Phys.* **1952**, *20*, 1809−1810.
(49) Whitmer, J. C. Energy-Distributions in Vibrating Systems - Choice of Coordinates. *J. Mol. Spectrosc.* **1977**, *68*, 326−328.
(50) Perdew, J.; Burke, K.; Ernzerhof, M. Generalized Gradient Approximation Made Simple. *Phys. Rev. Lett.* **1996**, *77*, 3865−3868.
(51) VandeVondele, J.; Krack, M.; Mohamed, F.; Parrinello, M.; Chassaing, T.; Hutter, J. QUICKSTEP: Fast and Accurate Density Functional Calculations Using a Mixed Gaussian and Plane Waves Approach. *Comput. Phys. Commun.* **2005**, *167*, 103−128.
(52) Lippert, G.; Hutter, J.; Parrinello, M. A Hybrid Gaussian and Plane Wave Density Functional Scheme. *Mol. Phys.* **1997**, *92*, 477−487.
(53) Goedecker, S.; Teter, M.; Hutter, J. Separable Dual-Space Gaussian Pseudopotentials. *Phys. Rev. B* **1996**, *54*, 1703−1710.
(54) Martyna, G. J.; Tuckerman, M. E. A Reciprocal Space Based Method for Treating Long Range Interactions in Ab Initio and Force-Field-Based Calculations in Clusters. *J. Chem. Phys.* **1999**, *110*, 2810−2821.
(55) Yoo, S.; Zeng, X. -C.; Xantheas, S. S. On the Phase Diagram of Water with Density Functional Theory Potentials: The Melting Temperature of Ice Ih with the Perdew−Burke−Ernzerhof and Becke−Lee−Yang−Parr Functionals. *J. Chem. Phys.* **2009**, *130*, 221102.
(56) Pascal, T. A.; Schärf, D.; Jung, Y.; Kühne, T. D. On the Absolute Thermodynamics of Water from Computer Simulations: A Comparision of First-Principles Molecular Dynamics, Reactive and Empirical Force Fields. *J. Chem. Phys.* **2012**, *137*, 244507.
(57) Schmidt, J.; VandeVondele, J.; Kuo, I. F. W.; Sebastiani, D.; Siepmann, J. I.; Hutter, J.; Mundy, C. Isobaric− Isothermal Molecular Dynamics Simulations Utilizing Density Functional Theory: An Assessment of the Structure and Density of Water at Near-Ambient Conditions J. *J. Phys. Chem. B* **2009**, *113*, 11959−11964.
(58) Jonchiere, R.; Seitsonen, A. P.; Ferlat, G.; Saitta, A. M.; Vuilleumier, R. van der Waals Effects in Ab Initio Water at Ambient and Supercritical Conditions. *J. Chem. Phys.* **2011**, *135*, 154503.
(59) Lin, I.-C.; Seitsonen, A. P.; Tavernelli, I.; Rothlisberger, U. Structure and Dynamics of Liquid Water from Ab Initio Molecular Dynamics-Comparison of BLYP, PBE, and revPBE Density Functionals with and without van der Waals Corrections. *J. Chem. Theory Comput.* **2012**, *8*, 3902−3910.
(60) Park, S.; Fayer, M. D. Hydrogen Bond Dynamics in Aqueous NaBr Solutions. *Proc. Natl. Acad. Sci. U.S.A.* **2007**, *104*, 16731−16738.
(61) Perry, A.; Ahlborn, H.; Space, B.; Moore, P. B. A Combined Time Correlation Function and Instantaneous Normal Mode Study of the Sum Frequency Generation Spectroscopy of the Water/Vapor Interface. *J. Chem. Phys.* **2003**, *118*, 8411−8419.
(62) Toth, R. Water Vapor Measurements between 590 and 2582 cm^{-1}: Line Positions and Strengths. *J. Mol. Spectrosc.* **1998**, *190*, 379−396.
(63) Kuyanov-Prozument, K.; Choi, M.; Vilesov, A. Spectrum and Infrared Intensities of OH-Stretching Bands of Water Dimers. *J. Chem. Phys.* **2010**, *132*, 014304.
(64) Devlin, J. P. Vibrational-Spectra and Point-Defect Activities of Icy Solids and Gas-Phase Clusters. *Int. Rev. Phys. Chem.* **1990**, *9*, 29−65.
(65) Scatena, L.; Brown, M.; Richmond, G. Water at Hydrophobic Surfaces: Weak Hydrogen Bonding and Strong Orientation Effects. *Science* **2001**, *292*, 908−912.
(66) Brown, M.; Walker, D.; Raymond, E.; Richmond, G. Vibrational Sum-Frequency Spectroscopy of Alkane/Water Interfaces: Experiment and Theoretical Simulation. *J. Phys. Chem. B* **2003**, *107*, 237−244.
(67) Mazzacurati, V.; Ricci, M. A.; Ruocco, G.; Signorelli, G.; Nardone, M.; Desantis, A.; Sampoli, M. Rovibrational Raman-Spectra and Polarizability Constants of the H_2S Molecule. *Mol. Phys.* **1985**, *54*, 1229−1240.
(68) Zhang, C.; Donadio, D.; Gygi, F.; Galli, G. First Principles Simulations of the Infrared Spectrum of Liquid Water Using Hybrid Density Functionals. *J. Chem. Theory. Comput.* **2011**, *7*, 1443−1449.
(69) Tian, C. S.; Shen, Y. R. Sum-Frequency Vibrational Spectroscopic Studies of Water/Vapor Interfaces. *Chem. Phys. Lett.* **2009**, *470*, 1−6.
(70) Raymond, E. A.; Tarbuck, T. L.; Brown, M. G.; Richmond, G. Hydrogen-Bonding Interactions at the Vapor/Water Interface Investigated by Vibrational Sum-Frequency Spectroscopy of HOD/H_2O/D_2O Mixtures and Molecular Dynamics Simulations. *J. Phys. Chem. B* **2003**, *107*, 546−556.
(71) Kühne, T. D.; Pascal, T. A.; Kaxiras, E.; Jung, Y. New Insights into the Structure of the Vapor/Water Interface from Large-Scale First-Principles Simulations. *J. Phys. Chem. Lett.* **2011**, *2*, 105−113.